Reverse Atom Transfer Radical Polymerization in Miniemulsion

Mei Li and Krzysztof Matyjaszewski*

Center for Macromolecular Engineering, Department of Chemistry, Carnegie Mellon University, 4400 Fifth Avenue, Pittsburgh, Pennsylvania 15213

Received January 27, 2003; Revised Manuscript Received May 20, 2003

ABSTRACT: Reverse atom transfer radical polymerization was successfully carried out in a miniemulsion system at 70 °C with a doubled solid content (≥20%) and $^1/_6$ amount of nonionic surfactant, Brij 98 (2.3 wt % based on monomer, or 0.58 wt % based on the aqueous phase), compared to the previously reported system. Hexasubstituted TREN/$CuBr_2$ and 2,2′-azobis[2-(2-imidazolin-2-yl)propane] dihydrochloride (VA-044) were employed as a highly active radical deactivator and a water-soluble initiator, respectively. Controlled polymerizations were demonstrated by attaining linear correlations between molecular weights and monomer conversion, and relatively narrow molecular weight distributions (<1.5). The resulting latexes showed good colloidal stability with an average particle size around 200−250 nm. Monomer droplet nucleation was proved to be the predominant nucleation mechanism in the system. The polymerization kinetics was governed mainly by the atom transfer equilibrium. Other parameters, such as ligand, surfactant, initiator, temperature, and deactivator (Cu^{II}) were investigated from both the polymerization kinetics and the colloidal stability points of view. The livingness and the end-functionality of the resulting polymers were demonstrated by the further chain extension study.

Introduction

Controlled/living radical polymerizations (CRP) provide a simple and versatile route to synthesize (co)-polymers with controlled molecular weights (and narrow distributions), well-defined compositions, desired architectures, and useful end-functionalities.[1,2] Stable free radical polymerization (SFRP),[3] atom transfer radical polymerization (ATRP),[4−6] and reversible addition−fragmentation chain transfer (RAFT) along with other degenerative chain transfer (DT) polymerization[7,8] are among the well-established methods for CRP. All of these methods are based on the rapid establishment of the activation/deactivation equilibrium, between a small fraction of growing radical chains and a large majority of dormant species, via either a reversible termination (SFRP and ATRP) or a reversible transfer (RAFT and DT) mechanism.[9] Extensive studies on CRP were conducted in homogeneous bulk and solution systems. However, the needs for commercialization of CRP techniques have directed the attention of research to the development of CRP processes in heterogeneous system, such as suspension, dispersion, and emulsion/miniemulsion. Related reviews of interest can be found elsewhere.[10−12] Among these aqueous dispersed systems, miniemulsion polymerization has become the primary approach for the application of CRP techniques (including SFRP,[13−22] ATRP,[23] RAFT,[24−29] and DT[30−32]) because its unique droplet nucleation minimizes the need of mass transport of the control agents (i.e., stable free radicals in SFRP, radical activator/deactivator species in ATRP, chain transfer agents in RAFT or DT) to the polymerization loci.

The earlier attempt[33] to apply copper-mediated ATRP in aqueous dispersed system using an anionic surfactant, sodium dodecyl sulfate (SDS), and a hydrophilic ligand, bipyridine, was not successful. However, upon the identification of some crucial experimental conditions,[34] such as using nonionic surfactant with certain HLB values (HLB = 20 W_{EO}/W_{TOTAL}, where W_{EO} is the weight of the hydrophilic part, and W_{TOTAL} is the total weight of the molecular) (e.g., Brij 98) and hydrophobic ligand (e.g., 4,4′-di(5-nonyl)-2,2′-bipyridine, dNbpy), ATRP was conducted successfully in aqueous dispersed media. Well-defined polymers, including poly(methyl methacrylate),[35,36] poly(*n*-butyl methacrylate),[23,34,37−39] poly(*n*-butyl acrylate),[34,37] polystyrene,[34] and block copolymers[40] were synthesized with narrow molecular weight distributions. However, it was found that the direct ATRP usually yielded micrometer-size particles with poor colloidal stability when using an oil-soluble initiator (i.e., ethyl 2-bromoisobutyrate, EB*i*B). A microsuspension, instead of an emulsion, polymerization mechanism was utilized to explain the phenomena. To improve the colloidal stability, a miniemulsion approach was applied,[23] where hydrophobic dNbpy, nonionic Brij 98, hexadecane, and water-soluble azo compound, 2,2′-azobis(2-methylpropionamide)dihydrochloride (V-50), were employed as ligand, surfactant, costabilizer, and normal free radical initiator, respectively. A controlled polymerization was demonstrated by a linear correlation between molecular weights and monomer conversion, and a relatively narrow molecular weight distribution (<1.5). The resulting latexes showed improved stability with an average size around 300 nm. However, a large amount of surfactant (13.5 wt % based on monomer) was employed to obtain stable latexes with a relatively low solid content (∼13%). Furthermore, a high surfactant concentration brings about complexity to the mechanism of miniemulsion polymerization due to the coexistence of micelles and submicrometer-sized monomer droplets, which will be further addressed in the results and discussion section.

In this article, we report a more practical ATRP miniemulsion system with a reasonable solid content (≥20%) and much lower surfactant concentration (2.3 wt % based on monomer or 0.58 wt % based on water). A new type of nitrogen-based tetradentate ligand, with higher catalytic activity and better cost/performance balance compared to dNbpy, was used. Considering the

* Corresponding author. E-mail: km3b@andrew.cmu.edu.

10.1021/ma034109d CCC: $25.00
Published on Web 07/11/2003

Scheme 1. General Scheme of a Reverse ATRP Process

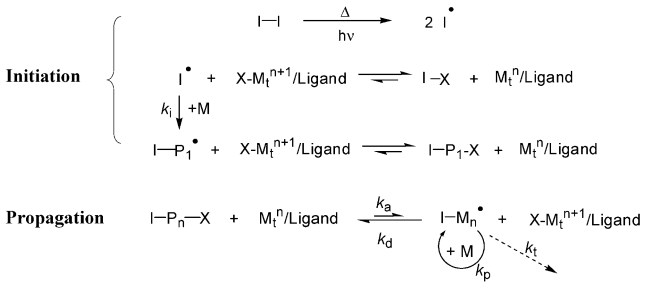

Table 1. Typical Recipe for a Reverse ATRP of BMA in Miniemulsion System[a]

monomer	BMA	5.0 g	400 equiv
ligand	EHA_6TREN	0.11 g	1 equiv
catalyst	$CuBr_2$	0.0197 g	1 equiv
costabilizer	hexadecane[b]	0.18 g	
surfactant	Brij 98[c]	0.115 g	
deionized water	H_2O	19.88 g	
water-soluble initiator	VA-044	0.0284 g	1 equiv

[a] Solid content = 20% (based on 100% conversion). [b] 3.6 wt % based on monomer. [c] 2.3 wt % based on monomer; 0.58 wt % based on water.

high sensitivity of the Cu^I/ligand catalyst complex to air, a reverse ATRP process (Scheme 1)[41,42] starting with a conventional thermal radical initiator (e.g., azo compound, VA-044) and Cu^{II}/ligand was adapted for the current study.

Experimental Section

Materials. *n*-Butyl methacrylate (BMA; Aldrich), *n*-butyl acrylate (BA, Aldrich), 2-ethylhexyl acrylate (EHA, Aldrich), and lauryl acrylate (LA, Aldrich) were purified by passing each compound through an inhibitor removal column filled with basic aluminum oxide (Aldrich), respectively. The monomers were stored at −5 °C for later use. 4,4′-Di(5-nonyl)-2,2′-bipyridine (dNbpy),[43] tris(2-bis(3-butoxy-3-oxopropyl)aminoethyl)amine (BA_6TREN),[44] and tris(2-bis(3-(2-ethylhexoxy)-3-oxopropyl)aminoethyl)amine (EHA_6TREN)[45] were synthesized according to previous published procedures, respectively. Tris-(2-bis(3-dodecoxy-3-oxopropyl)aminoethyl)amine (LA_6TREN) was prepared, via a slightly modified procedure in a reported work,[45] by further extending the reaction at 50 °C for another 24 h. $CuBr_2$ (Aldrich), tris(2-aminoethyl)amine (TREN, Aldrich), Brij 98 (Aldrich), NOIGEN RN20 (Montello), Hexadecane (Aldrich), and 2,2′-azobis[2-(2-imidazolin-2-yl)propane] dihydrochloride (VA-044, Wako Chem. Inc.) were used as received.

Miniemulsion Polymerization. A typical recipe for the preparation of miniemulsions is listed in Table 1. The radical deactivator ($CuBr_2$ and ligand), monomer, and the costabilizer (hexadecane) were mixed and heated with magnetic stirring at 60 °C for 10 min to form a homogeneous solution. After the reaction cooled to room temperature, the surfactant solution was added and the mixture was ultrasonified (Heat Systems Ultrasonics W-385 sonicator; output control at 8 and duty cycle at 70% for 2 min) in an ice bath to prevent a significant temperature rise resulting from sonification. The resulting miniemulsion exhibited good shelf life stability at room temperature, as evidenced by a lack of creaming or phase separation over 3 days of aging.

After homogenization, the miniemulsion was immediately transferred to a 25 mL Schlenk flask, where pure argon was bubbled through the miniemulsion for 30 min before it was immersed in an oil bath thermostated at 70 °C. The magnetic stirring speed was set at 700 rpm. Then, the polymerization was initiated by the injection of pre-deoxygenated initiator aqueous solution. Samples were withdrawn periodically via pre-degassed syringe to monitor the kinetics. Further chain extension reactions were performed as follows: a first-step miniemulsion polymerization via reverse ATRP process was carried out as described above; after the polymerization reached high conversion (>90%, monitored by GC), premixed and deoxygenated monomer and surfactant solution were continuously fed into reaction media via syringe pump at a controlled rate for a period of time. The reaction was continued to complete the polymerization.

Characterization. A small portion of the emulsion samples was dissolved in THF for measuring the monomer conversion using GC (Shimadzu GC-14A gas chromatograph). Samples for molecular weights analysis were dried in the vacuum oven, redissolved in THF, and analyzed using GPC, which was equipped with autosampler (Waters, 717 plus), HPLC pump at 1 mL/min (Waters, 515), and four columns (guard, 10^5 Å, 10^3 Å, and 100 Å; Polymer Standards Services) in series. Toluene was used as internal standards. A calibration curve based on linear poly(methyl methacrylate) standands was used in conjunction with a differential refractometer (Waters, 2410). The particle size was measured using dynamic light scattering (Malvern Zetasizer 3000HSA) in dilute solution.

Results and Discussion

The main objective of this work was to develop a more efficient and practical miniemulsion polymerization system that allows the application of ATRP technique in aqueous dispersed media. Qiu[46] examined the copper-mediated ATRP of BMA in emulsion/miniemulsion system in her thesis. To facilitate a successful ATRP, it was essential to have both the radical activator and deactivator available in the organic phase where the polymerization takes place. Thus, the selection of a suitable ligand became imperative. One of the roles that the ligand plays is adjusting the partitioning behavior of the metal complex, at both higher and lower oxidation states, between the oil phase and the aqueous phase. Only those ligands that exhibit sufficient hydrophobicity bring at least some activator (i.e., Cu^I) and deactivator (i.e., Cu^{II}) into organic phase to establish and maintain the atom transfer equilibrium between the growing radicals and the dormant species. Further, even with a very hydrophobic ligand, neither the Cu^I nor the Cu^{II} complex was restricted to the organic phase. Since a detailed partitioning study of metal complexes was reported elsewhere,[39] it would not be the focus of this article. Instead, the exploitation and examination of a new type of efficient ligand that can be applied to the ATRP in the dispersed system will be addressed. We will also discuss several other important parameters of ATRP in the miniemulsion system, such as the concentration of surfactant, initiator, and deactivator, as well as the temperature. In the last part of this article, the results from a chain extension study will be used to evaluate the livingness of the resulting polymers.

Nature of the Ligands. Pyridine derivatives with long alkyl substituents, such as dNbpy, were effectively employed as ligands for ATRP in emulsion and miniemulsion systems.[46] However, the catalytic activity of copper complex with dNbpy is rather low which requires high polymerization temperature and reduces the stability of monomer droplets/growing particles during the polymerization. Moreover, the elevated reaction temperature may result in the hydrolysis of alkyl halide end groups, which lead to uncontrolled polymerizations or polymers with less functional end groups. A new type of ligands that forms a catalyst complex with high activity and meets the requirements for the miniemulsion polymerization is demanded. It has been shown that nitrogen-based tetradentate ligands currently form the most efficient catalyst in bulk or solution ATRP.[47−51]

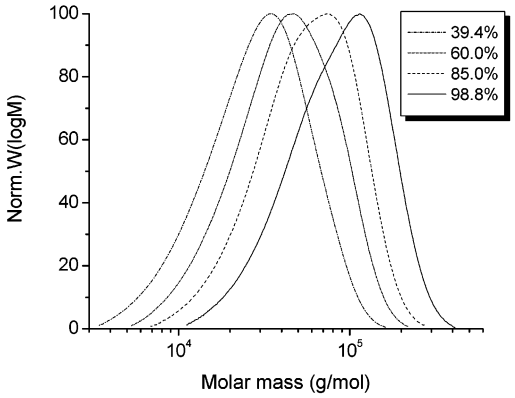

Figure 1. GPC chromatograms for a reverse ATRP of BMA in miniemulsion. $[BMA]_0/[CuBr_2-EHA_6TREN]_0/[VA\text{-}044]_0$ = 400/1/1; [Brij 98]/[hexadecane] = 2.3/3.6 wt % based on monomer; 20% solid content; reaction temperature = 70 °C.

Scheme 2. Synthesis of Hexasubstituted TREN Ligands via Michael Addition Reaction

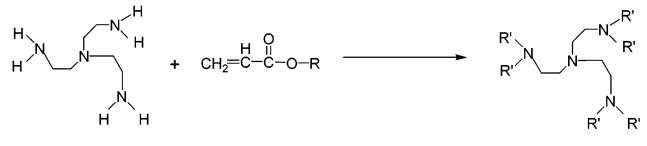

R' = CH_2CH_2COOR

R : Tris(2-bis(3-butoxy-3-oxopropyl)aminoethyl)amine (BA_6TREN)

Tris(2-bis(3-(2-ethylhexoxy)-3-oxopropyl)aminoethyl)amine (EHA_6TREN)

Tris(2-bis(3-dodecoxy-3-oxopropyl)aminoethyl)amine (LA_6TREN)

In addition, the structure of this type of ligands could be easily adjusted by the Michael addition of tris(2-aminoethyl)amine (TREN) and 6 equiv of an unsaturated reagent (such as acrylate) under mild conditions (e.g., room temperature), as shown in Scheme 2. A series of hexasubstituted TREN ligands bearing long acrylate substituents were synthesized, including BA_6TREN, EHA_6TREN, and LA_6TREN. The incorporation of *n*-butyl acrylate, 2-ethylhexyl acrylate, or lauryl acrylate increases the partitioning coefficient of the catalyst in the monomer phase, which could provide better control over the polymerizations by maintaining the atom transfer equilibrium in the growing polymer particles. However, the normal ATRP process faced handling problem, especially when applied to miniemulsion system, because of the high air sensitivity of Cu^I complex resulting from the use of these highly active ligands. Reverse ATRP, using more stable Cu^{II} complexes in the initiating step, would be a more convenient method allowing to overcome this handling problem.

Figure 1 shows the GPC traces of a typical reverse ATRP in BMA miniemulsion, where $CuBr_2/EHA_6TREN$ and VA-044 were employed as the catalytic system and the radical initiator, respectively. The clear shifts of molecular weights toward the higher values with conversion indicate a well-controlled polymerization. The kinetic plot and molecular weight evolution during the miniemulsion polymerizations using various hexasubstituted TREN ligands, as well as dNbpy ligand, are presented in Figure 2. Similar kinetic behavior, with relatively linear semilogarithmic plots, was observed when using BA_6TREN, EHA_6TREN, or LA_6TREN as ligand. The rate increase at the end of polymerization might due to the partitioning of deactivator (Cu^{II}/ligand) to the aqueous phase. The linear increase of molecular

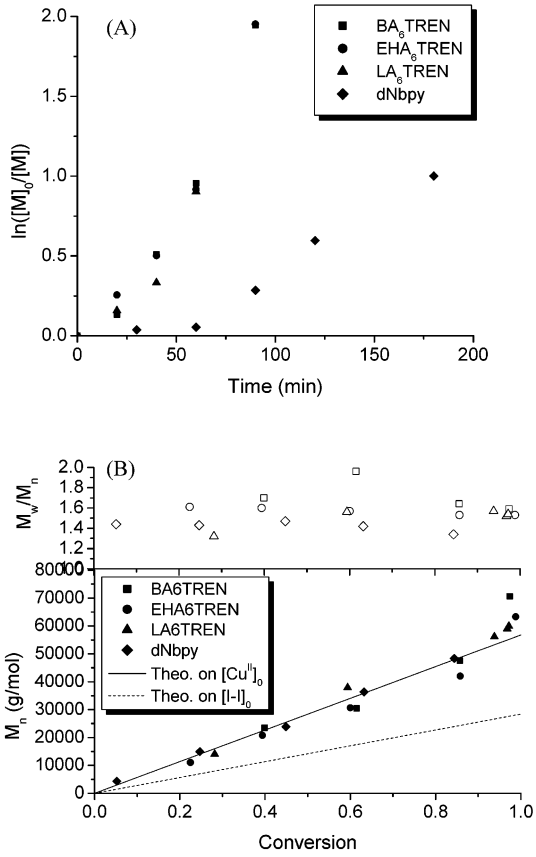

Figure 2. (A) First-order kinetic plots and (B) evolution of molecular weight and polydispersity vs conversion (filled symbols represent molecular weights; unfilled symbols represent polydispersity) for the reverse ATRP of BMA miniemulsions using various ligands. $[BMA]_0/[CuBr_2-ligand]_0/[VA\text{-}044]_0$ = 400/1/1; [Brij 98]/[hexadecane] = 2.3/3.6 wt % based on monomer; 20% solid content; reaction temperature = 70 °C. The theoretical molecular weights are calculated based on $[Cu^{II}]_0$ ($M_{n,\ theo.\ on\ [CuII]0} = M_0([M]_0/[Cu^{II}]_0) \times$ conversion, where M_0 is the molar mass of the monomer) and $[I-I]_0$ ($M_{n,\ theo.\ on\ [CuII]0} = M_0([M]_0/2\,f\,[I-I]_0) \times$ conversion, where f, the initiator efficiency, is assumed to be 1), respectively.

weight with conversion (Figure 2B) and clear shift of the entire distributions (Figure 1) indicate the "living" nature of the polymerizations. It was noted that there was no significant induction period when using TREN-based ligands. The induction period observed in the run using dNbpy as ligand (30−60 min shown in Figure 2A) was related to the time required for the generation of sufficient amount of initiating radicals by the decomposition of a radical initiator to reduce the deactivator concentration and reach the appropriate atom transfer equilibium.[39] The detectable conversion at the beginning of the polymerization is attributed to the formation of oligomeric radicals prior to the establishment of the atom transfer equilibrium. Theoretically, the number of living chains ($N_{theor,L.C.}$) is determined by initiator concentration ($N_{theor,L.C.} = N_A \times 2\,f\,[I-I]_0$, N_A is Avogadro's number and f is initiator efficiency) when $[Cu^{II}]_0 \geq 2\,f\,[I-I]_0$. However, in the case of $[Cu^{II}]_0 < 2\,f\,[I-I]_0$, the excess of the initiating radicals (if any) leads to the generation and termination of the oligomeric chains, which only contribute to the broadening of the molecular weight distribution but the number of living chains. Thus, the number of "real" living chains ($N_{L.C.}$) would be less than the theoretical value calculated by the initial radical concentration ($N_{L.C.} = N_{theor,L.C.} - N_{oligomeric\ chain}$). As shown in Figure 2B, the

Table 2. Particle Sizes of Latexes Prepared via Reverse ATRP in Miniemulsions

expt	ligand	[Brij 98] (wt %)[a]	temp (°C)	$[M]_0/[Cu^{II}]_0/[L]/[I-I]_0$	D_I[b] (nm)	PDI[c]
E52	BA_6TREN	2.3	70	400/1/1/1	206	1.18
E51	EHA_6TREN	2.3	70	400/1/1/1	212	1.01
E56	LA_6TREN	2.3	70	400/1/1/1	237	1.21
E87	dNbpy	2.3	70	400/1/2/1	261	1.43[d]
E18	LA_6TREN	13.3	60	400/1/1/1	151	1.01
E21	LA_6TREN	13.3	60	400/1/1/1	193	1.06
E25	LA_6TREN	13.3	60	400/1/1/1	212	1.04
E40	LA_6TREN	2.3	60	400/1/1/1	229	1.01
E44	LA_6TREN	2.3	60	400/1/1/1	242	1.16
E38	EHA_6TREN	13.3	60	400/1/1/1	188	1.84[e]
E49	EHA_6TREN	2.3	60	400/1/1/1	245	1.01
E57	EHA_6TREN	2.3	70	200/1/1/1	215	1.03
E58	EHA_6TREN	2.3	70	800/1/1/1	242	1.02
E60	EHA_6TREN	2.3	70	800/2/2/1	238	1.01
E63	EHA_6TREN	2.3	70	400/1.5/1.5/1	254	1.05

[a] On the basis of monomer; solid content (based on 100% conversion) is 20% at 2.3 wt % Brij 98, and 13.5% at 13.3 wt % Brij 98, respectively. [b] Intensity-average diameter measured by dynamic light scattering. [c] Polydispersity index = volume-average diameter (D_v)/number-average diameter (D_n). [d] Latex particles showed bimodal size distribution with two peaks at 53 nm (15% in area) and 264 nm (85% in area) in mean volume-average diameter, respectively. [e] Latex particles showed bimodal size distribution with two peaks at 61 nm (64% in area) and 210 nm (36% in area) in mean volume-average diameter, respectively.

experimental molecular weights agree relatively well with the theoretical values computed based on the number of chains corresponding to the initial concentration of deactivator (Cu^{II}/ligand) ($M_{n,theo} = M_0([M]_0/[Cu^{II}]_0) \times$ conversion, M_0 is the molar mass of the monomer) instead of the initiator concentration. The molecular weight distribution (M_w/M_n) of the resulting polymers are broader ($M_w/M_n \sim 1.5$) than that using $CuBr_2$/dNbpy complex as catalytic system ($M_w/M_n = 1.34$) at a same 1:1 ratio of $[Cu^{II}]_0/[I-I]_0$. It may be due to their different activities and partitioning coefficients. Polydispersities could be reduced at a high $[Cu^{II}]_0/[I-I]_0$ ratio, as discussed later.

From the colloidal point of view, no significant influence on the particle size (or the particle number) was observed when using various TREN-based ligands. This is consistent with the ideal case of miniemulsion polymerization where the particle number is determined only by the number of monomer droplets prior to the polymerization, which is a function of surfactant concentration. It was noteworthy that there was no coagulum throughout the course of polymerization at a 20% solid and 2.3 wt % (based on monomer) nonionic surfactant, Brij 98. The resulting latex particles have good colloidal stability, with the size around 200−250 nm and relatively low polydispersity (Table 2). Compared to the previously reported miniemulsion system,[23] the solid content has been increased to an acceptable level with the use of 6 times less surfactant.

After the initial success of using hexasubstituted TREN as ligand in a miniemulsion system via a reverse ATRP process, miscellaneous polymerizations were performed. The results are shown in Table 3. Well-controlled polymerizations were also achieved at 30% solid content, polymerizing *n*-butyl acrylate, and by using polymerizable surfactant, NOIGEN RN20, respectively. Little coagulum was found throughout the polymerizations.

Effect of Surfactant Concentration. Nonionic surfactants with a HLB value around 15 (e.g., Brij 97, Brij 98, and HV25) were found to be capable of providing better colloidal stability to the latex particles in aqueous dispersed ATRP.[46] A 13.3 wt % (based on monomer) sample of Brij 98 was initially used to prepare a miniemulsion.[23] However, experiments with the same recipe resulted in a poor reproducibility when LA_6TREN was employed as ligand (shown in Table 4). The molecular weights showed bimodal distributions in most of the cases. By monitoring the reaction kinetics, high molecular weight polymer ($M_n > 10^6$ g/mol) was produced primarily at the beginning of the reaction (<30% conversion) (Figure 3). This suggested that there were two polymerization mechanisms operating in the system, a conventional free radical polymerization accounting for the higher molecular weight polymer and a controlled radical polymerization for the lower one ($M_n \sim 10^4$ g/mol). Since a considerable number of micelles, together with submicrometer-sized monomer droplets, would exist in the miniemulsion system at such a high surfactant concentration, both micellar nucleation and droplet nucleation would occur after decomposition of the water-soluble initiator, VA-044. LA_6TREN is a highly hydrophobic ligand containing long hydrocarbon chains. Thus, metal complex formed with this ligand would be restricted in the monomer droplets upon homogenization of the oil and aqueous phases. Diffusion of the catalyst, LA_6TREN complexed with copper ion, between the droplets (or growing particles) would be highly retarded. As a result, the particles produced via micellar nucleation would undergo an uncontrolled conventional free radical polymerization due to the absence of copper complex as deactivator/activator. The controlled ATRP would only take place in the monomer droplets that contained LA_6TREN. To improve the control and minimize the interference from the presence of micelle, the surfactant concentration was dramatically decreased to 2.3 wt % (based on monomer). A well-controlled ATRP in a miniemulsion system (shown in Figure 2) was accomplished with little coagulum formed in the final latexes. The lack of high molecular weight moiety in the final polymer implied that the particles were produced predominately via droplet nucleation, where LA_6TREN complexed with Cu^{II} and Cu^{I} served as the deactivator/activator in the growing particles.

The effect of surfactant concentration was further investigated using EHA_6TREN as a ligand. Well-controlled polymerizations were achieved even at a high surfactant concentration. Molecular weights increased linearly with conversion at 13.3 and 2.3 wt % (based on monomer) Brij 98, respectively, as shown in Figure 4. This indicates that EHA_6TREN, with lower hydrophobicity and lower steric hindrance than LA_6TREN, might have sufficient diffusional capability through the aqueous phase to the growing particles, although it preferably partitioned in the organic (monomer) phase. Thus, controlled polymerizations might take place in particles generated by either micellar nucleation or droplet nucleation. The molecular weight is little affected by the amount of surfactant. The independence of molecular weight on the surfactant concentration was also observed in a nitroxide-mediated miniemulsion system.[52] Nevertheless, an increase in the polydispersity (Figure 4) at a high surfactant concentration would be related to the insufficient deactivation in a large number of growing radicals (polymerization loci). Since the solid contents are different in each case (13.5% at the higher

Table 3. Miscellaneous Miniemulsion Polymerizations via a Reverse ATRP Process[a]

monomer	[surfactant][b]	solid content[c] (%)	conversion (%)	$M_{n,\,theor}$ (g/mol)	$M_{n,\,sec}$ (g/mol)	M_w/M_n
BMA	Brij 98	20	98.8	56 100	63 300	1.53
BMA	Brij 98	30	98.7	56 100	60 400	1.52
BMA	NOIGEN RN20	20	91.0	51 700	49 200	1.55
BA	Brij 98	20	92.0	47 100	40 500	1.70

[a] $[M]_0/[CuBr_2-EHA_6TREN]_0/[VA\text{-}044]_0 = 400/1/1$; 2.3/3.6 wt % surfactant/costabilizer (hexadecane) based on monomer, respectively; Reaction temperature = 70 °C. [b] Brij 98: $C_{12}H_{25}(OC_2H_5)_{20}OH$; NOIGEN RN20:

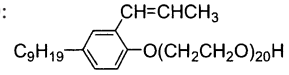

[c] On the basis of 100% conversion.

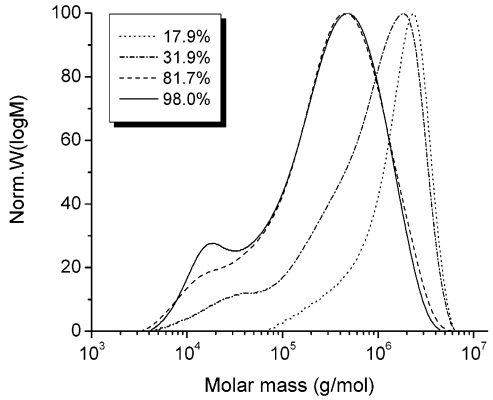

Figure 3. GPC chromatograms for the reverse ATRP of BMA in miniemulsion at a higher surfactant concentration (13.3 wt % Brij98 based on monomer), where LA_6TREN was used as ligand (Run E21). $[BMA]_0/[CuBr_2\text{-}LA_6TREN]_0/[VA\text{-}044]_0 = 400/1/1$; [hexadecane] = 3.6 wt % based on monomer; 13% solid content; reaction temperature = 60 °C.

Table 4. Reverse ATRP of BMA Miniemulsions[a] Using LA_6TREN as Ligand

[Brij 98] (wt %)[b]	expt	conversion (%)	$M_{n,sec}$ (g/mol)	$M_{n,theor}$[c] (g/mol)	M_w/M_n
13.3	E18	99.3	58 100	56 400	1.59
	E21	98.0	59 400	56 800	8.10[d]
	E25	100	33 400	56 800	9.29[d]
2.3	E40	65.3	32 600	37 100	1.59
	E44	100	57 900	56 800	1.61

[a] $[BMA]_0/[CuBr_2-LA_6TREN]_0/[VA\text{-}044]_0 = 400/1/1$; reaction temperature = 60 °C; Solid content (based on 100% conversion) is 20% at 2.3 wt % (based on monomer) Brij 98, and 13.5% at 13.3 wt % (based on monomer) Brij 98, respectively. [b] On the basis of monomer. [c] $M_{n,theo} = M_0([M]_0/[Cu^{II}]_0) \times$ conversion, where M_0 is the molar mass of the monomer. [d] Bimodal distribution. Two peaks were included in the calculation of M_w/M_n.

surfactant concentration vs 20% at the lower surfactant concentration), the effect of surfactant concentration on the polymerization rate cannot be quantitatively analyzed. Little effect was reported in nitroxide-mediated miniemulsion systems.[52,53]

When 13.3 wt % (based on monomer) surfactant was employed, the resulting latex particles showed bimodal size distribution (Table 2) with one peak around 60 nm and the other around 210 nm, which provided direct evidence for the presence of both micellar nucleation and droplet nucleation in miniemulsion system at a high surfactant concentration. The unimodal particle size, when using 2.3 wt % (based on monomer) surfactant, accounts for the predominant droplet nucleation mechanism.

Effect of Temperature. Temperature plays an important role in controlling the polymerization rate. In a reverse ATRP process, the decomposition rate of the normal radical initiator, the equilibrium constant

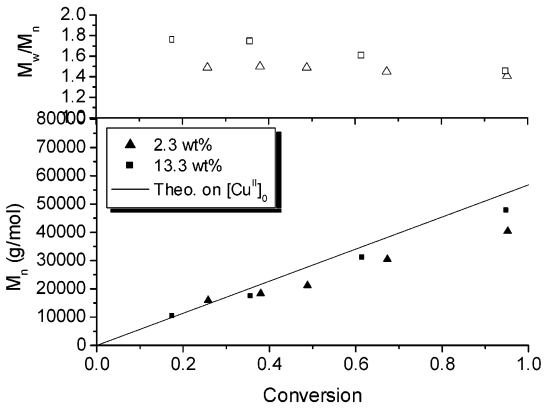

Figure 4. Evolution of molecular weight and polydispersity vs conversion (filled symbols represent molecular weights; unfilled symbols represent polydispersity) for the reverse ATRP of BMA in miniemulsion with different surfactant concentrations. $[BMA]_0/[CuBr_2-EHA_6TREN]_0/[VA\text{-}044]_0 = 400/1/1$; [hexadecane] = 3.6 wt % based on monomer; 20% solid content; reaction temperature = 60 °C. See Figure 2 for the calculation of theoretical molecular weights.

of the atom transfer reaction, and the propagation rate constant are all affected by temperature. From a colloid stability point of view, the stabilization of monomer droplets/growing particles becomes more difficult in a miniemulsion system at an elevated temperature. A primary motivation of this work is to develop an emulsion/miniemulsion ATRP system that can be operated at a relatively low temperature. In such a system, both the control over the polymerization and the preservation of the colloid stability would be fulfilled. Conversely, a low temperature may introduce a slow initiation process and a continuous supply of free radicals from a normal radical initiator in reverse ATRP, both of which lead to poorly controlled polymerizations. The use of an initiator with a low decomposition temperature, such as VA-044 (10 h $t_{1/2}$, temperature = 44 °C), and a highly active catalytic complex, such as $CuBr_2/EHA_6TREN$, would be a feasible strategy to approach the goal. Two polymerizations were carried out at 60 and 70 °C, respectively, as shown in Figure 5. Since the influence of temperature on the colloidal stability is not significant over this temperature range, the focus of discussion would be directed to the polymerization kinetics. As expected, a higher temperature led to a higher polymerization rate (Figure 5A). An apparent 30 min induction period was observed in the polymerization at 60 °C. It might result from the slower decomposition rate of VA-044 ($t_{1/2,60\,°C}$ = 60 min vs $t_{1/2,70\,°C}$ = 15 min) at a lower temperature. The molecular weights increase linearly with conversion and fairly fit the theoretical values. It is noted that the polydipersities of the resulting polymers are slightly lower at 60 °C. Plausibly, the temperature influences the partitioning behavior of the deactivator, Cu^{II}/ligand. A higher organic

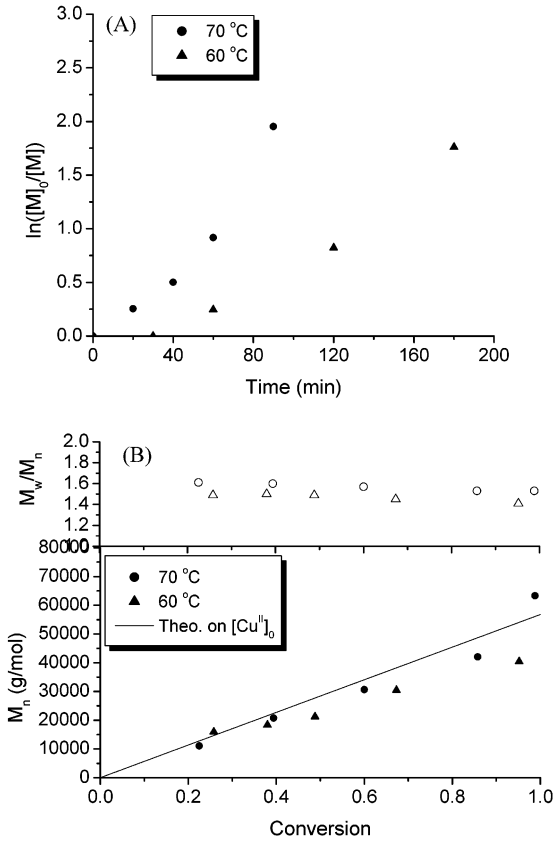

Figure 5. (A) First-order kinetic plots, and (B) evolution of molecular weight and polydispersity vs conversion (filled symbols represent molecular weights; unfilled symbols represent polydispersity) for the reverse ATRP of BMA in miniemulsion at different reaction temperatures. $[BMA]_0/[CuBr_2-EHA_6TREN]_0/[VA\text{-}044]_0 = 400/1/1$; [Brij 98]/[hexadecane] = 2.3/3.6 wt % based on monomer; 20% solid content. See Figure 2 for the calculation of theoretical molecular weights.

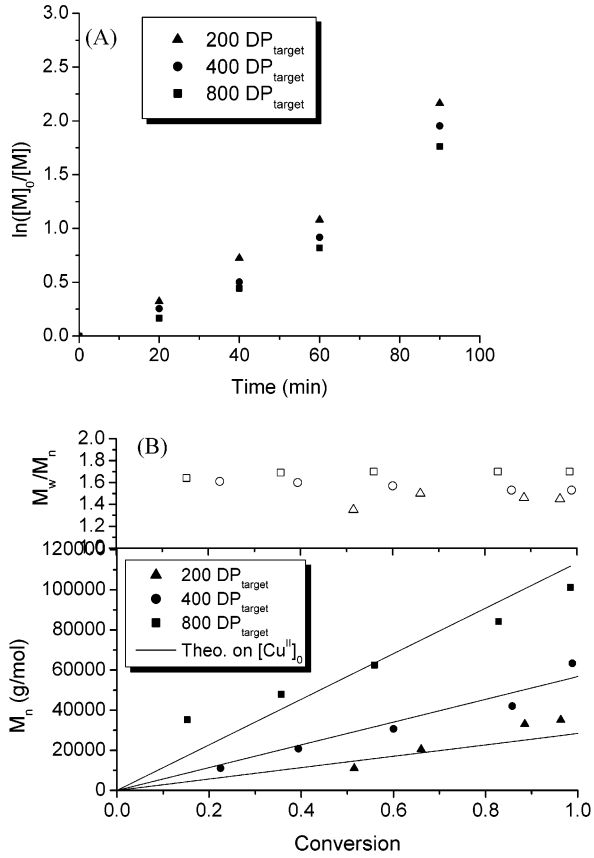

Figure 6. (A) First-order kinetic plots, and (B) evolution of molecular weight and polydispersity vs conversion (filled symbols represent molecular weights; unfilled symbols represent polydispersity) for the reverse ATRP of BMA in miniemulsion at various $[M]_0/[I-I]$ ratio. $[BMA]_0/[CuBr_2-EHA_6TREN]_0/[VA\text{-}044]_0 = 200$, 400, or 800/1/1; [Brij98]/[hexadecane] = 2.3/3.6 wt % based on monomer; 20% solid content; reaction temperature = 70 °C. See Figure 2 for the calculation of theoretical molecular weights.

partitioning of the Cu^{II} species at a lower temperature favors the control over the polymerization, resulting in a narrowing of the molecular weight distribution.

Effect of Initiator Concentration. The water-soluble azo initiator, VA-044, was employed in this series of experiments as a normal free radical initiator to start the reverse ATRP process in miniemulsion system. The ATRP initiator, an alkyl halide, is generated in situ by the deactivation reaction of radicals produced by VA-044 with Cu^{II}/ligand complex. Thus, the variation of VA-044, as well as Cu^{II}/ligand complex, corresponds to the changes in the concentration of the resulting normal ATRP initiator (i.e., alkyl halide, RX). Usually, the ratio of monomer to initiator ($[M]_0/[RX]_0$) was varied by targeting polymers with different degrees of polymerizations (DPs) in ATRP. From our previous miniemulsion studies, the molecular weight ($M_{n,theo}$) depends on the initial concentration of Cu^{II} species ($[Cu^{II}]_0$) at a ratio of $[I-I]_0/[Cu^{II}]_0 = 1{:}1$. Keeping this ratio of $[I-I]_0/[Cu^{II}]_0$ constant, the reverse ATRP was performed by varying the ratio of monomer to initiator, hence Cu^{II}/ligand complex, with a targeted degree of polymerization ($DP_{target} = [M]_0/[Cu^{II}]_0 = [M]_0/[I-I]_0$) at 200, 400, and 800, respectively. The linear dependence of $\ln([M]_0/[M])$ vs reaction time (Figure 6 A) and the linear development of the molecular weights with monomer conversion (Figure 6B) indicated a controlled polymerization in each case. Usually, a higher initiator concentration results in a larger number of growing chains, and therefore, a faster rate of polymerization. However, radical termination occurs more rapidly as well, leading to decreased initiator efficiency and consequently the formation of a larger excess of Cu^{II} species. The two phenomena have opposite effects on the rate of polymerization, which depends on the ratio of $[Cu^{I}][\text{growing chains}]/[Cu^{II}]$. The slightly faster polymerization rate at a higher initiator concentration (Figure 6A) suggests that the growing radicals are slightly larger in number despite the enhanced termination rate at meantime. The broader molecular weight distribution (M_w/M_n in Figure 6B) at a lower $[I-I]_0$, hence $[Cu^{II}]$, indicates the insufficient deactivation or formation of dead chains in the course of polymerization when targeting a higher degree of polymerization.

The final particles size is little affected by the initiator concentration. It was in the range 210−240 nm for each case (Table 2). The lack of dependence of the final particle size, hence number of particles, on the initiator concentration is a strong indication for a predominant droplet nucleation mechanism in current miniemulsion system.[54]

Effect of Initial Concentration of Deactivator (Cu^{II}/Ligand). Cu^{II} species are essential for achieving a controlled radical polymerization in a reverse ATRP process, as illustrated in Scheme 1. Sufficient deactivation reactions are not only to start the controlled polymerization by an in situ generating ATRP initiator,

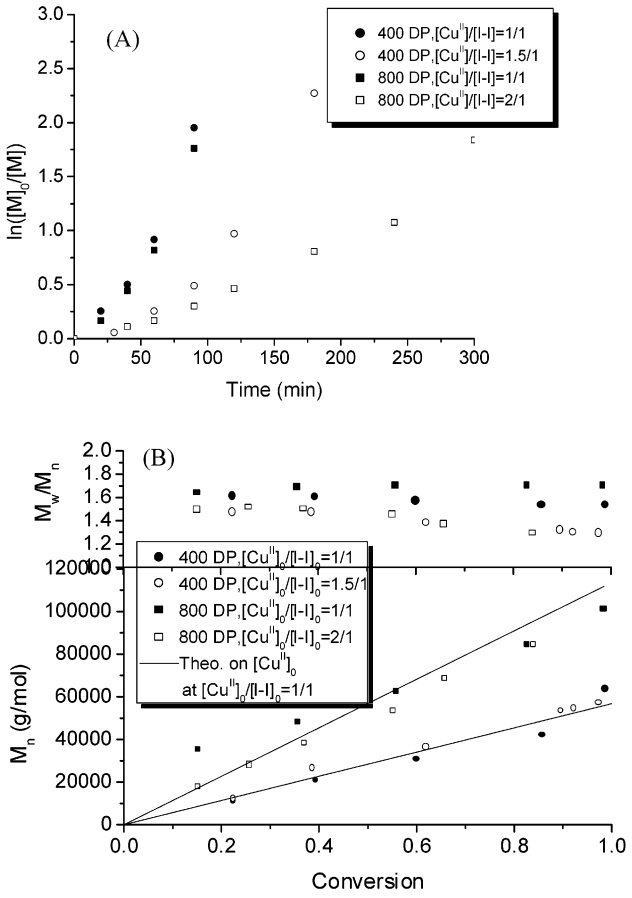

Figure 7. (A) First-order kinetic plots, and (B) evolution of molecular weight and polydispersity vs conversion for the reverse ATRP of BMA in miniemulsion at different $[Cu^{II}]/[I-I]$ ratio. [Brij98]/[hexadecane] = 2.3/3.6 wt % based on monomer; 20% solid content; reaction temperature = 70 °C; for 400 DP: $[BMA]_0/[VA\text{-}044]_0 = 400/1$; for 800 DP: $[BMA]_0/[VA\text{-}044]_0 = 800/1$. See Figure 2 for the calculation of theoretical molecular weights.

alkyl halide, but also to enable the controlled polymerization by reversible deactivation of growing chains. As shown in Figure 7 A, the initial ratio of Cu^{II}/ligand complex to initiator concentration has a great effect on the kinetics of a reverse ATRP reaction. The polymerization is much slower when excess Cu^{II} species was employed, which is in agreement with the rate law of ATRP.[42,43] For a reverse ATRP, the amount of initial Cu^{II} species should be high enough to deactivate all the free radicals generated from the normal free radical initiator in order to conduct a well-controlled polymerization. Apparently, a relatively higher amount of Cu^{II} resulted in a better control over polymerization (in terms of molecular weight evolution, shown in Figure 7B), especially at the beginning of the polymerization (i.e., in the case of $DP_{target} = 800$). This suggests that the aqueous partitioning of Cu^{II} species should be considered, especially at a high targeted DP, where less deactivator is employed. The molecular weight distribution is narrower with higher amount of Cu^{II} (M_w/M_n = 1.29 at $[Cu^{II}]_0/[VA\text{-}044]_0 = 1.5{:}1$ and $DP_{target} = 400$, or $[Cu^{II}]_0/[VA\text{-}044]_0 = 2{:}1$ and $DP_{target} = 800$ in Figure 7B). This is related to slower propagation and high partitioning of the deactivator, Cu^{II}/EHA_6TREN, in the organic phase, which affords more efficient reversible deactivation of the growing chains. Thus, more Cu^{II} species are needed for a better-controlled polymerization and a final polymer with relatively lower polydispersity.

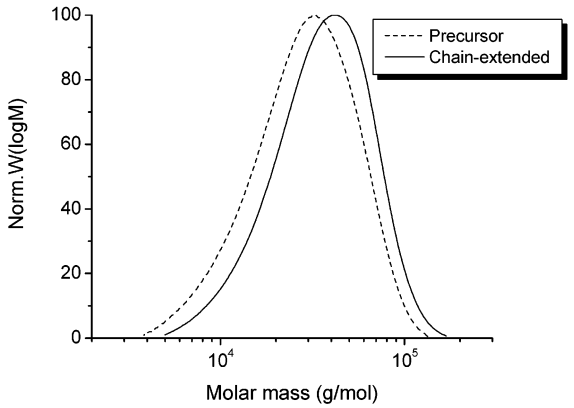

Figure 8. GPC traces of precursor polymer and chain-extended polymer obtained by chain extension via reverse ATRP in miniemulsion. Same reaction conditions as in Table 5.

Table 5. Chain Extension of Miniemulsion Latexes via a Reverse ATRP Process[a]

	mol wt		particle size	
polymer latexes	$M_{n,sec}$ (g/mol)	M_w/M_n	D_v (nm)	polydispersity
1st stage seed	21 000	1.51	251	1.01
after chain extension	27 000	1.46	271	1.01

[a] First-stage seed-latexes preparation conditions: $([BMA]/[CuBr_2\text{-}BA_6TREN]_0/[VA\text{-}044]_0 = 200/1/1$; [Brij 98]/[Hexadecane] = 2.3/3.6 wt % based on monomer; 20% solid content (based on 100% conversion); reaction temperature = 70 °C. Second-stage feeding conditions: 1.5 g of BMA and 0.0345 g of Brij 98 at a feed rate of 0.056 mL/minute for 30 min. The reaction was continued for another 30 min to complete the polymerization.

Chain Extension. To check the chain end functionality of the polymers prepared via reverse ATRP in miniemulsion and explore the potential for block copolymerization in this system, a chain extension study was performed by feeding the monomer and surfactant solution into the resulting polymer latexes. Feeding of the second-stage monomer started at 98.3% conversion of the first-stage monomer. The GPC traces of the precursor and chain-extended polymers are shown in Figure 8. A clear shift of the GPC traces after chain extension indicates the livingness of the polymers in the seed latexes. The experimental data from GPC analysis showed $DP_{precursor,expt} = 149$ and $DP_{chain-extended,expt} = 191$, respectively, both of which deviated from the theoretical values ($DP_{precursor,theor} = 200$ and $DP_{chain-extended,theor} = 260$). However, the extent of chain extension, calculated by $(DP_{chain-extended} - DP_{precursor})/DP_{precursor}$, were comparable for the theoretical (= 30%) and experimental (= 28%) values. The volume-average diameter of the final particle size is 271 nm (Table 5), which is also close to the theoretical value of 274 nm ($D_v = D_{v0}\,(1 + (W_{add}/W_0))^{1/3}$, where D_{v0} is the volume-average diameter of the seed particles; W_0 and W_{add} are the mass of the seed and the feed monomer, respecitively). This result provides additional evidence for the success of the chain extension reaction.

Conclusion

This work demonstrated a successful reverse atom transfer radical polymerization in the miniemulsion system with a doubled solid content (≥20%) and one-sixth of the amount of surfactant, Brij 98 (2.3 wt % based on monomer, or 0.58 wt % based on aqueous

phase), compared to the previously reported system. A series of hydrophobic hexasubsituted TREN (i.e., BA_6TREN, EHA_6TREN, and LA_6TREN)/$CuBr_2$ complexes, with high catalytic activity and better cost/performance balance than 2,2′-bipyridine derivatives (i.e., dNbpy), were employed as catalytic systems. The use of such ligands and a radical initiator with fast decomposition rate (i.e., water-soluble azo compound, VA-044) enables a well-controlled polymerization at a relatively low temperature (i.e., ≤ 70 °C), which favors the colloidal stability of the monomer droplets/growing particles in the course of the polymerization. Controlled polymerizations were demonstrated by linear semilogarithmic plots, linear correlations between molecular weights, and monomer conversions, as well as relatively low molecular weight distributions ($M_w/M_n < 1.5$). The independence of the particle size, hence the number of particles, on initiator concentration strongly indicated a predominant droplet nucleation mechanism in this miniemulsion system. There was little coagulum observed throughout the polymerization, and the resulting latex particles showed good colloidal stability. The average particle sizes were in the range of 200−250 nm with relatively low polydispersity. The above system showed a "living" nature for ATRP of several monomers (i.e., *n*-butyl methacrylate and *n*-butyl acrylate), surfactants (i.e., Brij 98 and NOIGEN RN20), at a higher solid content (i.e., 30%), and at various degrees of polymerization ($DP_{designed}$ = 200, 400, 800).

The polymerization kinetics was mainly governed by atom transfer equilibrium. The higher the initiator concentration and the lower the deactivator concentration, the faster the polymerization rate, which is in agreement with the rate law of ATRP.

Acknowledgment. Mr. J. Gromada is acknowledged for the synthesis of EHA_6TREN. Financial support from the EPA, Grant R-82958001, and the CRP consortia of Carnegie Mellon University is greatly appreciated.

References and Notes

(1) Matyjaszewski, K.; Davis, T. P., Eds. *Handbook of Radical Polymerization*; John Wiley & Sons Inc.: New York, 2002.
(2) Davis, K. A.; Matyjaszewski, K. *Adv. Polym. Sci.* **2002**, *159*, 2; Coessens, V.; Pintauer, T.; Matyjaszewski, K. *Prog. Polym. Sci.* **2001**, *26*, 337.
(3) Hawker, C. J.; Bosman, A. W.; Harth, E. *Chem. Rev.* **2001**, *101*, 3661.
(4) Wang, J. S.; Matyjaszewski, K. *J. Am. Chem. Soc.* **1995**, *117*, 5614.
(5) Matyjaszewski, K.; Xia, J. *Chem. Rev.* **2001**, *101*, 2921.
(6) Kamigaito, M.; Ando, T.; Sawamoto, M. *Chem. Rev.* **2001**, *101*, 3689.
(7) Matyjaszewski, K.; Gaynor, S. G.; Wang, J. S. *Macromolecules* **1995**, *28*, 2093.
(8) Chiefari, J.; Rizzardo, E. In *Handbook of Radical Polymerization*; Matyjaszewski, K., Davis, T. P., Eds.; John Wiley & Sons Inc.: New York, 2002; p 629.
(9) Matyjaszewski, K. *ACS Symp. Ser.* **2000**, *768*, 2.
(10) Qiu, J.; Charleux, B.; Matyjaszewski, K. *Prog. Polym. Sci.* **2001**, *26*, 2083.
(11) Cunningham, M. F. *Prog. Polym. Sci.* **2002**, *27*, 1039.
(12) Asua, J. M. *Prog. Polym. Sci.* **2002**, *27*, 1283.
(13) Prodpran, T.; Dimonie, V. L.; Sudol, E. D.; El-Aasser, M. S. *Macromol. Symp.* **2000**, *155*, 1.
(14) Pan, G.; Sudol, E. D.; Dimonie, V. L.; El-Aasser, M. S. *Macromolecules* **2001**, *34*, 481.
(15) MacLeod, P. J.; Barber, R.; Odell, P. G.; Keoshkerian, B.; Georges, M. K. *Macromol. Symp.* **2000**, *155*, 31.
(16) Keoshkerian, B.; MacLeod, P. J.; Georges, M. K. *Macromolecules* **2001**, *34*, 3594.
(17) Keoshkerian, B.; Szkurhan, A. R.; Georges, M. K. *Macromolecules* **2001**, *34*, 6531.
(18) Tortosa, K.; Smith, J.; Cunningham, M. F. *Macromol. Rapid Commun.* **2001**, *22*, 957.
(19) Cunningham, M. F.; Xie, M.; McAuley, K. B.; Keoshkerian, B.; Georges, M. K. *Macromolecules* **2002**, *35*, 59.
(20) Benoit, D.; Grimaldi, S.; Robin, S.; Finet, J. P.; Tordo, P.; Gnanou, Y. *J. Am. Chem. Soc.* **2000**, *122*, 5929.
(21) Farcet, C.; Lansalot, M.; Charleux, B.; Pirri, R.; Vairon, J. P. *Macromolecules* **2000**, *33*, 8559.
(22) Farcet, C.; Charleux, B.; Pirri, B. *Macromolecules* **2001**, *34*, 3823.
(23) Matyjaszewski, K.; Qiu, J.; Tsarevsky, N. V.; Charleux, B. *J. Polym. Sci., Polym. Chem. Ed.* **2000**, *38*, 4724.
(24) Le, T. P.; Moad, G.; Rizzardo, E.; Thang, S. H. WO9801478, 1998.
(25) Moad, G.; Chiefari, J.; Chong, Y. K.; Krstina, J.; Mayadunne, R. T. A.; Postma, A.; Rizzardo, E.; Thang, S. H. *Polym. Int.* **2000**, *49*, 993.
(26) de Brouwer, H.; Tsavalas, J. G.; Schork, F. J.; Monteiro, M. J.; Yase, K. *Macromolecules* **2000**, *33*, 9239.
(27) Tsavalas, J. G.; Schork, F. J.; de Brouwer, H.; Monteiro, M. J. *Macromolecules* **2001**, *34*, 3938.
(28) Butte, A.; Storti, G.; Morbidelli, M. *Macromolecules* **2001**, *34*, 5885.
(29) Lansalot, M.; Davis, T. P.; Heuts, J. P. A. *Macromolecules* **2002**, *35*, 7582.
(30) Butte, A.; Storti, G.; Morbidelli, M. *Macromolecules* **2000**, *33*, 3485.
(31) Lansalot, M.; Farcet, C.; Charleux, B.; Vairon, J.; Pirri, R. *Macromolecules* **1999**, *32*, 7354.
(32) Farcet, C.; Lansalot, M.; Pirri, R.; Vairon, J. P.; Charleux, B. *Macromol. Rapid Commun.* **2000**, *21*, 921.
(33) Makino, T.; Tokunaga, E.; E.; H.-E. T. *Polym. Prepr. (ACS, Div. Polym. Chem.)* **1998**, *39* (1), 288.
(34) Gaynor, S. G.; Qiu, J.; Matyjaszewski, K. *Macromolecules* **1998**, *31*, 5951.
(35) Jousset, S.; Qiu, J.; Matyjaszewski, K.; Granel, C. *Macromolecules* **2001**, *34*, 6641.
(36) Chambard, G.; de Man, P.; Klumperman, B. *Macromol. Symp.* **2000**, *150*, 45.
(37) Qiu, J.; Gaynor, S. G.; Matyjaszewski, K. *Macromolecules* **1999**, *32*, 2872.
(38) Matyjaszewski, K.; Qiu, J.; Shipp, D. A.; Gaynor, S. G. *Macromol. Symp.* **2000**, *150*, 15.
(39) Qiu, J.; Pintauer, T.; Gaynor, S. G.; Matyjaszewski, K.; Charleux, B.; Vairon, J. *Macromolecules* **2000**, *33*, 7310.
(40) Matyjaszewski, K.; Shipp, D. A.; Qiu, J.; Gaynor, S. G. *Macromolecules* **2000**, *33*, 2296.
(41) Wang, J. S.; Matyjaszewski, K. *Macromolecules* **1995**, *28*, 7572.
(42) Xia, J.; Matyjaszewski, K. *Macromolecules* **1997**, *30*, 7692.
(43) Matyjaszewski, K.; Patten, T. E.; J.; X. *J. Am. Chem. Soc.* **1997**, *119*, 674.
(44) Zeng, F.; Shen, Y.; Zhu, S.; Pelton, R. *Macromolecules* **2000**, *33*, 1628.
(45) Gromada, J.; Matyjaszewski, K. *Polym. Prepr. (Am. Chem. Soc., Div. Polym. Chem.)* **2002**, *43* (2), 195.
(46) Qiu, J. Ph.D. Dissertation, Carnegie Mellon University: Pittsburgh, PA, 2000.
(47) Xia, J.; Gaynor, S. G.; Matyjaszewski, K. *Macromolecules* **1998**, *31*, 5958.
(48) Xia, J.; Matyjaszewski, K. *Macromolecules* **1997**, *30*, 7697.
(49) Queffelec, J.; Gaynor, S. G.; Matyjaszewski, K. *Macromolecules* **2000**, *33*, 8629.
(50) Gromada, J.; Matyjaszewski, K. *Macromolecules* **2001**, *34*, 7664.
(51) Qiu, J.; Matyjaszewski, K.; Thouin, L.; Amatore, C. *Macromol. Chem. Phys.* **2000**, *201*, 1625.
(52) Pan, G.; Sudel, E. D.; Dimonie, V. L.; El-Aasser, M. S. *Macromolecules* **2002**, *35*, 6915.
(53) Charleux, B. *Macromolecules* **2000**, *33*, 5358.
(54) Blythe, P. J.; Morrison, B. R.; Mathauer, K. A.; Sudol, E. D.; El-Aasser, M. S. *Langmuir* **2000**, *16*, 898.

MA034109D